coatings

MDPI

Article

Antibacterial Activity of Electrodeposited Copper and Zinc on Metal Injection Molded (MIM) Micropatterned WC-CO Hard Metals

Christopher K. Dawari [1], Marianne Gunell [2,3], Kari Mönkkönen [4], Mika Suvanto [1] and Jarkko J. Saarinen [1,*]

[1] Department of Chemistry, University of Eastern Finland, 80101 Joensuu, Finland; christopher.dawari@uef.fi (C.K.D.); mika.suvanto@uef.fi (M.S.)
[2] Department of Clinical Microbiology, Turku University Hospital, 20521 Turku, Finland; marianne.gunell@tyks.fi
[3] Department of Medical Microbiology and Immunology, University of Turku, 20500 Turku, Finland
[4] Karelia University of Applied Sciences, 80200 Joensuu, Finland; kari.monkkonen@karelia.fi
* Correspondence: jarkko.j.saarinen@uef.fi

Abstract: Antibacterial activity of electrodeposited copper and zinc both on flat and micropatterned hard metal tungsten carbide-cobalt (WC-Co) specimens was studied. Tribological wear was applied on electrodeposited specimens: coatings were completely removed from flat surfaces whereas only top of the micropillars was exposed to wear for the micropatterned specimens protecting the functional metal coating in between the micropillars. The growth of *Staphylococcus aureus* (*S. aureus*) Gram-positive bacterial species was studied on the specimens using a touch test mimicking bacterial transfer from the surfaces. Copper coated specimens prevented bacterial growth completely independent of wear or surface structure, i.e., even residual traces of copper were sufficient to prevent bacterial growth. Zinc significantly suppressed the bacterial growth both on flat and micropatterned specimens. However, adhesion of zinc was low resulting in an easy removal from the surface by wear. The micropatterned zinc specimens showed antibacterial activity as electrodeposited zinc remained intact on the sample surface between the micropillars. This was sufficient to suppress the growth of *S. aureus*. On the contrary, the flat zinc coated surfaces did not show any antibacterial activity after wear. Our results show that micropatterned hard metal specimens can be used to preserve antibacterial activity under tribological wear.

Keywords: antibacterial activity; electrodeposition; *Staphylococcus aureus*; Gram-positive bacteria; copper; zinc; metal injection molding (MIM); tribological wear

Citation: Dawari, C.K.; Gunell, M.; Mönkkönen, K.; Suvanto, M.; Saarinen, J.J. Antibacterial Activity of Electrodeposited Copper and Zinc on Metal Injection Molded (MIM) Micropatterned WC-CO Hard Metals. *Coatings* **2022**, *12*, 485. https://doi.org/10.3390/coatings12040485

Academic Editors: Joaquim Carneiro and László A. Péter

Received: 18 February 2022
Accepted: 30 March 2022
Published: 4 April 2022

1. Introduction

Antibacterials have emerged in history as one of the most reliable forms of chemotherapy in medicine. Statistics show that high human morbidity and mortality rates have been reduced significantly through control of infectious diseases using antibacterial agents [1]. Metal based antibacterials, particularly the d-block transition metals, have provided lasting health care benefits especially in relation to communicable diseases [2]. For example, respiratory face masks impregnated with copper oxide have been successfully used in reducing human infectious influenza A virus infections [3]. Human immunodeficiency virus type 1 (HIV-1) in a culture medium was inactivated by copper-based filters [4]. If proven safe, such filters could be a significant contributor to reduce the spread of the virus through breast feeding and blood transfers [4]. Copper impregnated fibers in textile fabrics have also been reported to decrease the spread of bacteria in a clinical setting [5] and the risk of foot ulceration in patients with type 2 diabetes [6]. Copper surface has also shown microbicidal potency against *Salmonella enterica* and *Campylobacter jejuni*, which are common causative agents of foodborne diseases, particularly in poultry and poultry products [7]. Copper and

zinc are also used as nutrient supplements in animal feeds to enhance growth [8,9]. These trace elements can promote the growth of livestock by suppressing gut pathogens [10]. Porous clay-based ceramic stones embedded with submicron copper particles were used to disinfect water contaminated with *Staphylococcus aureus* (*S. aureus*) and *Klebsiella pneumoniae* bacteria [11]. Copper has also shown antibacterial activity against viable vegetative cells of *Clostridium difficile*, which is the main cause for antibiotic-associated diarrhea [12]. A typical zinc-based antibacterial agent has also exhibited potential inhibitory effect against oral pathogenic bacteria [13].

Typically, bacteria can tolerate Cu coated surfaces on a timescale from a few minutes to hours [2]. Cellular toxicity of copper is also reported as a factor of its ability to undergo a redox recycling between its cupric (Cu^{2+}), and cuprous (Cu^{1+}) ions. In the presence of a biological reductase such as ascorbate and plasma membrane, Cu^{2+} ions undergo reduction to Cu^{1+} ions in oxidation-reduction reactions. The Cu^{1+} has the capacity to break down hydrogen peroxide via Fenton reaction to produce reactive oxygen radicals which can inactivate biological molecules such as DNA, lipids, and proteins [14,15].

Contamination of touch surfaces such as doorknobs and push plates on doors in hospitals settings is a major source of spread of nosocomial pathogens and hospital-acquired infections (HAIs) [16]. Steel doorknobs and clinical equipment have been functionalized with more potent metal based antibacterial agents. However, most of these antibacterial surface wear with time. Hence, there is an urgent need to develop surfaces with structures that will reduce the effect of wearing of antibacterial agents.

In recent years several approaches have been presented combining structured materials with antibacterial activity such as micropatterned aluminum surfaces [17] or zinc [18] that also inhibit superhydrophobic character and thus reduce adhesion of bacteria. Alternatively, biomimetic approaches have been presented combining surface chemistry and topography for antibacterial activity [19,20]. However, typically such micropatterned surfaces are prone to wear. Durability of micropatterns can be improved using, for example, microscale armor [21].

In this study a solution to wear is proposed by combining surface micropatterning with antibacterial metals. Regular micropillars on the specimen surface functioned as the wear-carrying pads whereas the areas between the micropillars remained intact. Square patterned round shaped micropillars in one-to-one ratio were studied, i.e., 200 μm diameter micropillars with a spacing of 200 μm. This ratio guarantees both protection of the areas between the pillars against wear and a sufficient amount of functional metal between the pillars for antibacterial activity against *S. aureus*. Thus, even materials with low adhesion can be utilized in a micropatterned set-up as they are not directly exposed to wear.

Here we examined electrodeposited copper and zinc both on flat and micropatterned hard metal WC-Co specimens. The aim of the micropatterned structure was to protect the deposited antibacterial metal on the surface against wear. The coatings on the flat surfaces were completely removed by a tribological wear whereas in the micropatterned specimens only the top of the pillars was exposed to wear, leaving the coating intact in between the micropillars. The growth of *S. aureus* Gram-positive bacterial species was characterized on the specimens using the touch test mimicking bacterial transfer from the surfaces. The bacterial colony forming units (CFUs) were calculated from the blood agar plates. The micropatterned specimens showed that zinc remained on the sample surface between the pillars even after wear with significantly suppressed growth of *S. aureus*.

2. Materials and Methods

2.1. Sample Preparation

Round-shaped micropillars in a square lattice as presented in Figure 1a were created on hard metal specimens by a microrobot technique combined with metal injection molding (MIM). A 200 μm size tungsten carbide needle (Fodesco Ltd., Lehmo, Finland), was assembled to the pitching arm of a micro-robot (Mitsubishi rp-1ah robot 1, Mitsubishi, Tokyo, Japan) to create micropits on a 0.25 mm thick nickel foil (64 mm × 12 mm, 99.9%).

Pitch locations on the nickel foil were controlled at equidistant separation of 200 µm from the edges. The created nickel mold insert was used to fabricate micropatterned hard metal specimens (WC-Co, WC0.8Co13.5, Z360, PolyMIM GmbH, Polymer-Group, Sobernheim, Germany) with the exact negative of the square lattice micropits by metal injection molding (MIM). For details of the WC-Co material used, see Refs. [22,23] in which SEM-EDS imaging (Hitachi S-4800, Tokyo, Japan) of the WC-Co hard metal specimens verified two distinct phases with WC grains mixed in a Co phase [23].

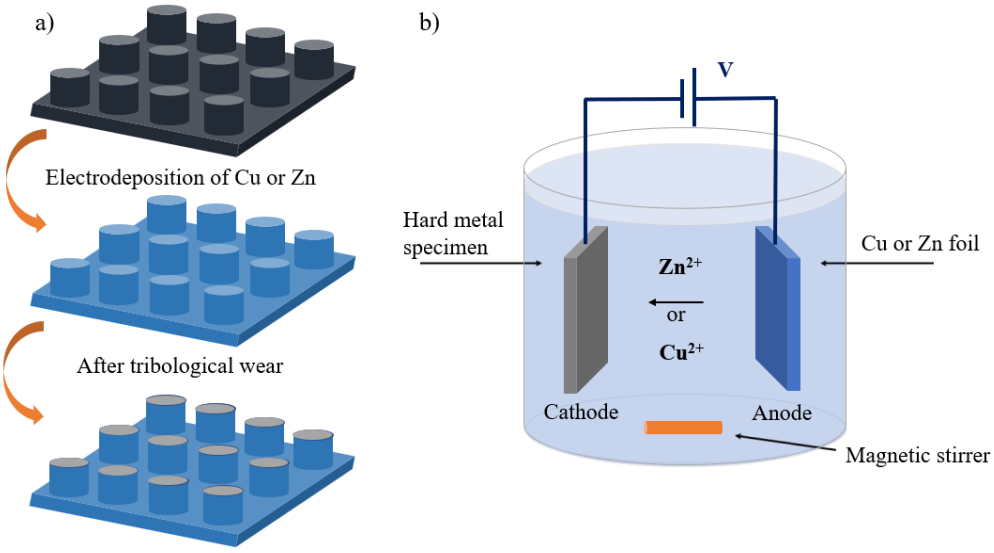

Figure 1. Schematic figure of (**a**) protective pillars against tribological wear and (**b**) the used electrodeposition setup.

The used micro-compounder was HAAKE Minijet II (Thermo Fisher Scientific, Karlsruhe, Germany). Injection of WC-Co feedstock into the mold cavity was carried out at a cylinder temperature of 191 °C having an injection pressure of 750 bar and injection time of 3 s. The heating tool temperature was set to 60 °C. The green part obtained after injection molding was debonded in a hot water bath at a constant temperature of 60 °C overnight. The specimens were then dried in a temperature-programmed oven at a constant temperature of 100 °C for 2 h to obtain the brown part. The brown part was densified through a sintering process to an elevated temperature of 1369 °C at 180 °C/h for 40 min in a high-temperature furnace (HTK 8 MO/16-1G, Carbolite/Gero, Carbolite Gero Ltd., Neuhausen, Germany) in a N_2 atmosphere before cooling to room temperature. For additional details of the sample preparation, see Ref. [22].

2.2. Electrodeposition of Copper and Zinc

Electrodeposition on both flat and micropatterned hard metal specimens were carried out in a simple electrolytic bath in a 100 mL glass beaker. The electrolytic system was set at a current of 0.15 A for 1 h treatment time. Electrodepositions of zinc and copper were carried out using zinc (II) acetate (anhydrous, 99.99%, Sigma-Aldrich GmbH, Germany) and copper (II) sulphate (anhydrous, 98%, Acros Organics, Espania) solutions, respectively. Next, 0.2 M equimolar solutions of each electrolyte were prepared by dissolving their calculated weighted masses in 90 mL of deionized water. The hard metal specimens were connected to the negative terminal of the electrolytic system as cathode. A 3.0 mm thick zinc foil (>99.99%, 25 × 25 mm^2, Goodfellow, Huntingdon, UK), and a 2.0 mm copper foil (>99.99%, Goodfellow, Huntingdon, UK) were connected to the positive terminal of the electrolytic system as an anode with the aid of crocodile clips as shown in Figure 1b.

Electrodeposition was carried out in a single-anode set-up. Ions from the positive anode (copper or zinc) were transferred into the electrolyte solution by oxidative loss of electrons. Positive metal ions were driven by electric potential onto the negative electrode;

in this case the hard metal specimens were coated with metal layer. It is noteworthy that uneven coating may be formed during electrodeposition. However, for antibacterial functionality uniformity of coating is not required.

2.3. Tribological Wear

Flat and micropatterned zinc and the copper coated specimens were subjected to wear on a CSM tribometer (CSM Instruments SA, Peseux, Switzerland; tribometer model S/N 18-347). Wearing of the surface coatings was carried out using a special pin attached with an approximately 1 cm^2 rubber band. An abrasive paper (P100) was attached to the rubber band to aid the surface wear. The aim was to remove the metal coatings completely from the flat specimens. The micropatterned specimens were exposed to the same wear conditions. This resulted in removal of the coatings on top of the pillars as schematically shown in Figure 1a. However, the coatings below and around the micropillars were left intact as the pillars served as protective weight-carrying structures.

2.4. Surface Morphology Characterization

The surface structure of the hard metal specimens after electrodepositions and specimens after tribological wear was characterized by field emission scanning electron microscope (FE-SEM, Hitachi S-4800, Tokyo, Japan) coupled with the electron dispersive x-ray (EDS) spectroscope for identification of elements. Secondary electron (SE) detector (Hitachi, Tokyo, Japan) was used for surface imaging and X-ray detector (Hitachi, Tokyo, Japan) for EDS imaging. Acceleration voltage of 10 kV was used throughout the imaging.

2.5. Antibacterial Activity of Copper and Zinc Coatings

Antibacterial activity of electrodeposited coatings was characterized using a touch test method [24] that mimics bacterial transfer from surfaces. Gram-positive *Staphylococcus aureus* (*S. aureus*, ATCC 29213) bacterial strain was diluted to 0.5 McFarland standard that corresponds to approximately 1.8×10^8 colony forming units (CFUs) per ml. Next, 50 µL of the prepared suspension was applied on the sample surface, and was incubated for 24 h at room temperature (RT). The sample surface was brought in contact with blood agar plate (tryptic soy agar W/5% SB (II); BD, Franklin Lakes, NJ, USA) for 30 s. The blood agar plates were incubated for 24 h at +37 °C after touching with the sample surface. The CFUs were then calculated from the blood agar plates.

The touch test assay was performed three times with *S. aureus* for each specimen. Mean and SD values were calculated for each trial. The error bars were neglected in plotting as no variation was observed between parallel measurements for each sample. The used touch test culture method was semiquantitative in nature, and the CFUs were calculated directly from the blood agar surface. A 95% confidence interval was used throughout the antibacterial testing between different specimens.

3. Results and Discussion

3.1. Characterization of Electrodeposited Metal Coatings

EDS SEM linescan images of the flat specimens are presented in Figure 2. They have been electrodeposited either with copper (Figure 2A) or zinc (Figure 2B). It is clearly seen that the EDS image of the copper coated specimen shows a larger variation in the deposition, i.e., more peaks and valleys were present compared to the zinc-coated specimens. This suggests that there is a more uniform deposition of zinc on the specimen surface. In addition, the zinc coatings can be thicker than copper. This may be associated with a faster deposition rate of zinc compared to copper. The zinc coating also appeared more porous with larger deposits than the copper coating.

3.2. Protective Micropillars with Electrodeposited Copper Coatings

Figure 3 shows the protective WC-Co micropillars with electrodeposited copper before and after tribological wear. Figure 3A,C show the EDS linescan images on top (A) and in

between (C) the copper electrodeposited micropillars. The yellow dashed lines indicate the position along which the counts for copper atoms (displayed by a blue line) have been measured. Figure 3B,D shows the specimens after tribological wear. Figure 3A displays that there was copper both on top and in between the micropillars. This implied a comparative amount of copper coatings both on top of the pillars and in between the pillars. However, after the wearing process, the linescans shows almost flat or less distinct peaks on top of the pillars, but highly distinct peaks at the areas between the pillars. This confirmed that sufficient residual amount of copper remained in between the micropillars. Thus, the micropillars functioned as protective structures for the coatings as expected. Vertical linescans were taken between the micropillars both before and after tribological wearing shown in Figure 3C,D, respectively. These confirmed that the coatings were preserved as there is no significant variation between the linescans in between the pillars. The vertical linescans were used between the micropillars due to shading effect of these micropillars in the horizontal direction (due to the location of the X-ray detector in the used SEM setup) in which no peaks were observed in the areas between the micropillars.

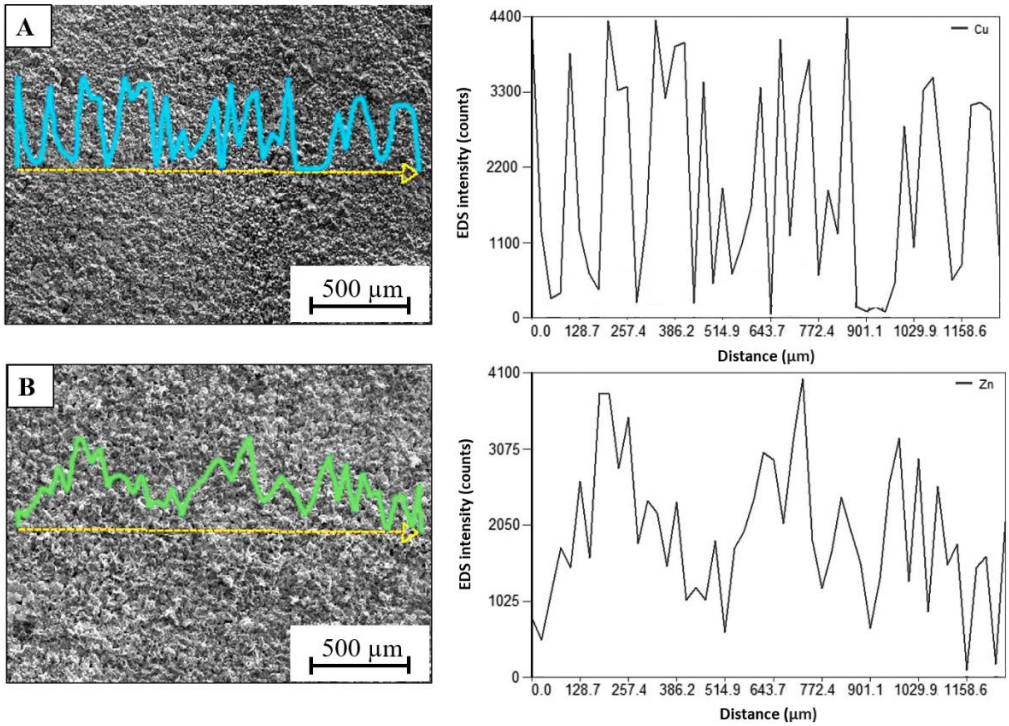

Figure 2. X-ray linescan spectra of electrodeposited (**A**) Cu (in cyan) and (**B**) Zn (in green) on flat hard metal specimens with the corresponding EDS intensity counts for various elements along the yellow dashed lines.

3.3. Protective Micropillars with Electrodeposited Zinc Coatings

Figure 4 presents EDS images of the zinc-coated micropatterned specimens before and after tribological wear. The yellow dashed lines indicate the position along which the counts for zinc atoms (displayed by blue lines) have been measured. The horizontal EDS linescan shows a comparable amount of clustered zinc both on top of the pillars and in between the pillars in Figure 4A. After wearing in Figure 4B, zinc on top of the pillars was almost completely removed, leaving only small residual traces as shown by the linescan. Comparing the vertical linescans between the pillars in Figure 4C,D before and after tribological wearing, it can be deduced that the residual amount of zinc on the specimen surface between the pillars did change significantly after wear. However, after the wear, compact clusters of zinc coating were observed and zinc debris was captured and unevenly distributed along the entire sample surface between the pillars. It can be concluded that the micropillars function as protective micropatterned structure similar to the copper coatings. However, a clear

difference in morphology of Zn and Cu deposits on the sample surface was observed when comparing Figures 3 and 4 as Zn formed larger clusters.

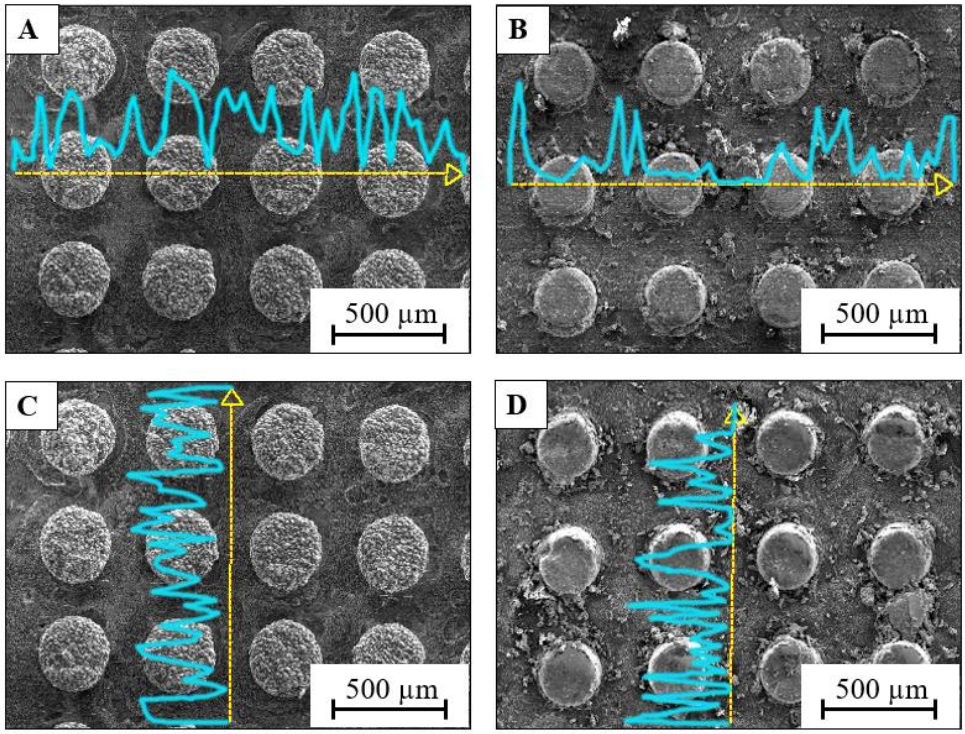

Figure 3. X-ray linescans (Cu EDS intensity count in cyan curves along the yellow dashed lines) of electrodeposited copper on 200 µm micropillar hard metal specimens before (**A**) and (**C**) and after (**B**) and (**D**) tribological wear.

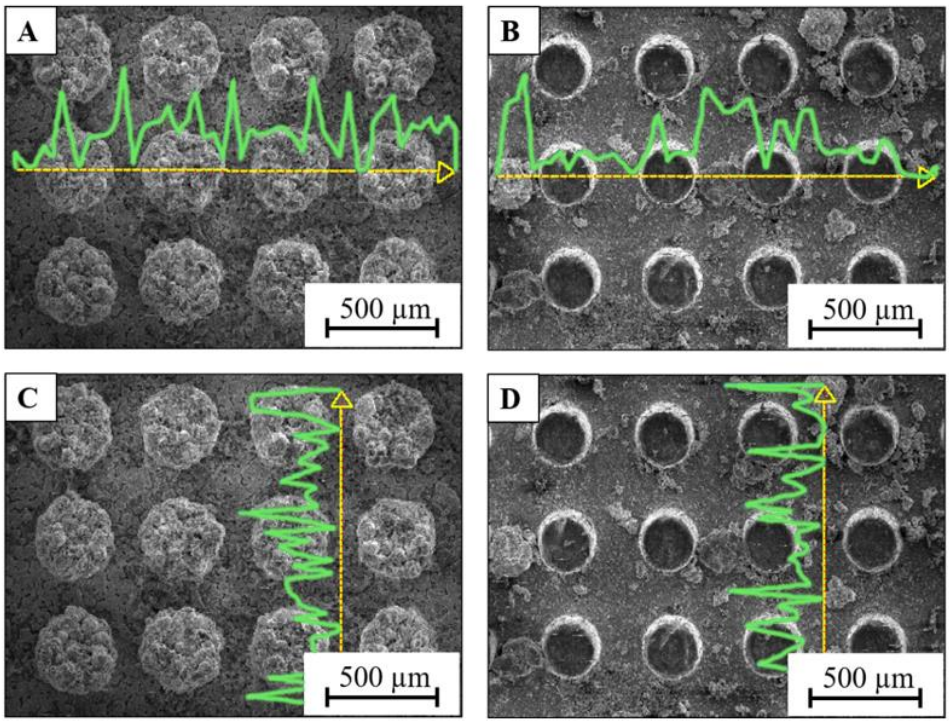

Figure 4. X-ray linescans (Zn EDS intensity count in green curves along the yellow dashed lines) of electrodeposited zinc on 200 µm micropillar hard metal specimens before (**A**) and (**C**) and after (**B**) and (**D**) tribological wear.

3.4. Antibacterial Activity of Copper and Zinc Coatings

Growth of *S. aureus* Gram-positive bacteria was studied using a touch test method on reference and electrodeposited specimens both on flat and micropatterned surfaces. The number of bacterial colony-forming units (CFUs) were calculated from the sample surfaces. The bacterial touch test results are displayed in Figure 5 for flat (A) and micropatterned (B) specimens. The corresponding bacterial colonies on blood agar are presented on top of Figure 5A,B. Figure 5A shows the bacterial CFUs on reference and zinc and copper electrodeposited flat specimens before and after tribological wear, whereas Figure 5B shows the corresponding results on micropatterned specimens. No antibacterial activity against *S. aureus* was observed on the reference WC-Co specimens independent of the surface structure. On the contrary, no growth was observed on the copper specimens independent of surface wear and structure. Even residual traces of copper on the worn flat surface were sufficient to completely remove the bacterial growth. On the zinc-coated specimens, bacterial growth was suppressed significantly independent of surface structure before wear. However, the zinc-coated flat specimens displayed no antibacterial activity after wear, similar to the reference specimens. On the contrary, for the micropatterned specimens the growth of *S. aureus* was completely inhibited by zinc even after wear. This may be associated with the fragmentation and distribution of smaller zinc clusters and debris that was captured between the micropillars after wear as displayed in Figure 4B,D. This is consistent with a previous study [25] on antibacterial activity of ZnO on five different microbial strains, including *S. aureus*. The study also revealed that smaller particle sizes, large specific area, and increased porosity increased antibacterial activity of ZnO. Particle size dependency of zinc based antibacterial agents has also been studied in previous studies [15,26,27]. In our study, the morphology of the zinc coatings was observed to have large clusters in between the micropillars. During wear these clusters were worn into smaller clusters and isolated zinc debris was formed between the pillars. This further explains the protective and preservative role of the micropatterned structures for less potent antibacterial agents than copper, whose antibacterial activity depends more on the amount of the antibacterial agent.

As a summary, complete removal to *S. aureus* growth was observed by copper surfaces both before and after wear. This was not a surprise even on a worn flat specimen since copper is generally known for high antibacterial activity even at low dosages [2]. Residual amount of zinc on the flat specimen after wear was not sufficient to reduce the bacterial growth compared to unworn specimens. This suggests that the antibacterial activity of zinc against *S. aureus* depends on the zinc concentration on the sample surface [28]. We can also conclude that the antibacterial activity of zinc against *S. aureus* on surfaces is less than copper. Thus, zinc does have capacity to reduce the growth of *S. aureus* but zinc coatings are also easily removed from flat surfaces. Micropatterned specimens confirmed that zinc remained on the sample surface in between the pillars and can thus provide long term antibacterial activity even under wear.

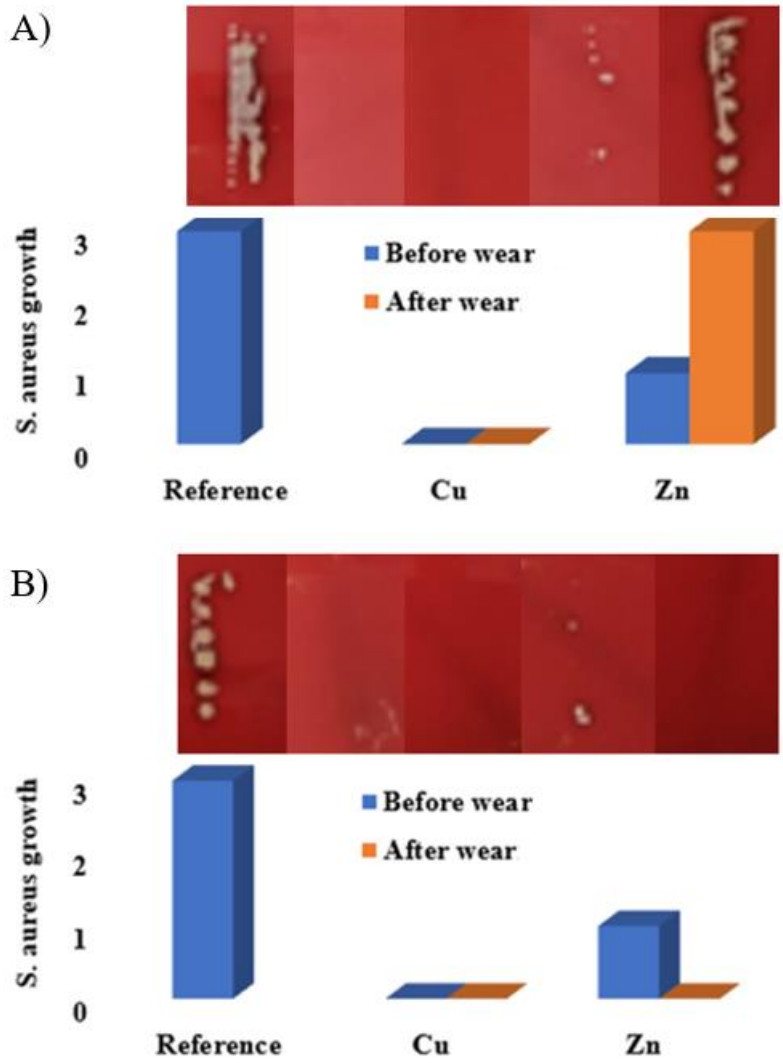

Figure 5. Growth of *S. aureus* after 24 h incubation on reference, Zn and Cu electrodeposited on (**A**) flat and (**B**) micropatterned hard metal specimens with the corresponding bacterial colonies on blood agar. Growth labels of *S. aureus* are related to bacterial colony-forming units as follows: 0 (no growth), 1 (10^3–10^4 CFU), 2 (10^4–10^5 CFU) and 3 (>10^5 CFU), respectively.

4. Conclusions

In this study, copper and zinc were electrodeposited on flat and micropatterned hard metal WC-Co specimens. The electrodeposited specimens were tribologically worn, which resulted in a complete removal of the functional coating on flat specimens with only residual traces remaining on the surface. Similar wearing conditions were applied to the specimens with micropillars that removed the antibacterial metal only from the top of the pillars, but the coatings in between the micropillars were protected from the wear.

The growth of *S. aureus* Gram-positive bacterial species was characterized on the reference, copper, and zinc electrodeposited flat and micropatterned specimens. The results showed no antibacterial activity on reference WC-Co specimens independent of surface patterning. The copper specimens completely suppressed the bacterial growth independent of surface wear and patterning. It can be concluded that even residual traces of copper on the surface after wear were sufficient to completely inhibit the bacterial growth. On the contrary, zinc can also suppress the growth of *S. aureus* but zinc has a lower adhesion than copper and can thus easily be removed from the flat surface. Micropatterned zinc coated specimens confirmed that zinc remained on the sample surface in between the pillars in sufficient amounts that can completely inhibit the growth of *S. aureus*.

We believe that these results can be used to design solutions that can tolerate long-term wear without losing antibacterial activity, which can find applications, for example, in the hospital environment in the future. The design of micropatterning can be controlled by varying the shape of micropillars (round, square, diamond) and their filling fraction for enhanced surface characteristics and antibacterial activity against both Gram-positive and negative bacteria. We plan to return to these aspects in a future communication.

Author Contributions: C.K.D.: investigation, writing—original draft; M.G.: investigation; K.M.: conceptualization, funding acquisition, project administration, resources; M.S.: conceptualization, funding acquisition, project administration, resources, supervision, writing—review and editing; J.J.S.: conceptualization, project administration, supervision, writing—review and editing. All authors have read and agreed to the published version of the manuscript.

Funding: We gratefully acknowledge the Business Finland/ERDF (European Regional Development Fund) project "MIM Components for Harsh Conditions, Grant agreement 7929/31/2019" for financial support. J.J.S. acknowledges the Academy of Finland funding (339 554) and the Academy of Finland Flagship for Photonics Research and Innovation (PREIN, decision no. 320 166).

Institutional Review Board Statement: Not applicable.

Informed Consent Statement: Not applicable.

Data Availability Statement: The data presented in this study are available in the article. The data presented in this study are also available upon request from the corresponding author.

Conflicts of Interest: The authors declare no conflict of interest.

References

1. Aminov, R.I. A brief history of the antibiotic era: Lessons learned and challenges for the future. *Front. Microbiol.* **2010**, *1*, 134. [CrossRef]
2. Turner, R.J. Metal-based antimicrobial strategies. *Microb. Biotechnol.* **2017**, *10*, 1062–1065. [CrossRef] [PubMed]
3. Borkow, G.; Zhou, S.S.; Page, T.; Gabbay, J. A novel anti-influenza copper oxide containing respiratory face mask. *PLoS ONE* **2010**, *5*, e11295. [CrossRef] [PubMed]
4. Borkow, G.; Lara, H.H.; Covington, C.Y.; Nyamathi, A.; Gabbay, J. Deactivation of human immunodeficiency virus type 1 in medium by copper oxide-containing filters. *Antimicrob. Agents Chemother.* **2008**, *52*, 518–525. [CrossRef] [PubMed]
5. Gabbay, J.; Borkow, G.; Mishal, J.; Magen, E.; Zatcoff, R.; Shemer-Avni, Y. Copper oxide impregnated textiles with potent biocidal activities. *J. Ind. Text.* **2006**, *35*, 323–335. [CrossRef]
6. Borkow, G.; Gabbay, J. Putting copper into action: Copper-impregnated products with potent biocidal activities. *FASEB J.* **2004**, *18*, 1728–1730. [CrossRef]
7. Faúndez, G.; Troncoso, M.; Navarrete, P.; Figueroa, G. Antimicrobial activity of copper surfaces against suspensions of Salmonella enterica and Campylobacter jejuni. *BMC Microbiol.* **2004**, *4*, 1–7. [CrossRef] [PubMed]
8. Monteiro, S.C.; Lofts, S.; Boxall, A.B.A. Pre-assessment of environmental impact of zinc and copper used in animal nutrition. *EFSA Support. Publ.* **2017**, *7*, 74E. [CrossRef]
9. Amachawadi, R.G.; Shelton, N.W.; Shi, X.; Vinasco, J.; Dritz, S.S.; Tokach, M.D.; Nelssen, J.L.; Scott, H.M.; Nagaraja, T.G. Selection of fecal enterococci exhibiting tcrB-mediated copper resistance in pigs fed diets supplemented with copper. *Appl. Environ. Microbiol.* **2011**, *77*, 5597–5603. [CrossRef] [PubMed]
10. Jacob, M.E.; Fox, J.T.; Nagaraja, T.G.; Drouillard, J.S.; Amachawadi, R.G.; Narayanan, S.K. Effects of feeding elevated concentrations of copper and zinc on the antimicrobial susceptibilities of fecal bacteria in feedlot cattle. *Foodborne Pathog. Dis.* **2010**, *7*, 643–648. [CrossRef] [PubMed]
11. Drelich, A.J.; Miller, J.; Donofrio, R.; Drelich, J.W. Novel durable antimicrobial ceramic with embedded copper sub-microparticles for a steady-state release of copper ions. *Materials* **2017**, *10*, 775. [CrossRef]
12. Wheeldon, L.J.; Worthington, T.; Lambert, P.A.; Hilton, A.C.; Lowden, C.J.; Elliott, T.S.J. Antimicrobial efficacy of copper surfaces against spores and vegetative cells of Clostridium difficile: The germination theory. *J. Antimicrob. Chemother.* **2008**, *62*, 522–525. [CrossRef] [PubMed]
13. Fang, M.; Chen, J.H.; Xu, X.L.; Yang, P.H.; Hildebrand, H.F. Antibacterial activities of inorganic agents on six bacteria associated with oral infections by two susceptibility tests. *Int. J. Antimicrob. Agents* **2006**, *27*, 513–517. [CrossRef]
14. Valko, M.; Morris, H.; Cronin, M. Metals, Toxicity and Oxidative Stress. *Curr. Med. Chem.* **2005**, *12*, 1161–1208. [CrossRef] [PubMed]
15. Jiang, W.; Mashayekhi, H.; Xing, B. Bacterial toxicity comparison between nano- and micro-scaled oxide particles. *Environ. Pollut.* **2009**, *157*, 1619–1625. [CrossRef]

16. Santo, C.E.; Taudte, N.; Nies, D.H.; Grass, G. Contribution of copper ion resistance to survival of Escherichia coli on metallic copper surfaces. *Appl. Environ. Microbiol.* **2008**, *74*, 977–986. [CrossRef]
17. Mandal, P.; Shishodia, A.; Ali, N.; Ghosh, S.; Arora, H.S.; Grewal, H.S.; Ghosh, S.K. Effect of topography and chemical treatment on the hydrophobicity and antibacterial activities of micropatterned aluminium surfaces. *Surf. Topogr. Metrol. Prop.* **2020**, *8*, 025017. [CrossRef]
18. Özcana, S.; Açıkbaş, G.; Açıkbaş, N.Ç. Induced superhydrophobic and antimicrobial character of zinc metal modified ceramic wall tile surfaces. *Appl. Surf. Sci.* **2018**, *438*, 136–146. [CrossRef]
19. Dolid, A.; Gomes, L.C.; Mergulhão, F.J.; Reches, M. Combining chemistry and topography to fight biofilm formation: Fabrication of micropatterned surfaces with a peptide-based coating. *Coll. Interfaces B Biointerfaces* **2020**, *196*, 111365. [CrossRef]
20. Yoo, C.H.; Jo, Y.; Shin, J.H.; Jung, S.; Na, J.-G.; Kang, T.; Lee, J.S. Hierarchical membrane integration of shear stress-resistant nanoparticles and biomimetic micropatterns for ultrahigh and durable biofouling resistance. *Chem. Eng. J.* **2022**, *432*, 134363. [CrossRef]
21. Wang, D.; Sun, Q.; Hokkanen, M.J.; Zhang, C.; Lin, F.-Y.; Liu, Q.; Zhu, S.-P.; Zhou, T.; Chang, Q.; He, B.; et al. Design of robust superhydrophobic surfaces. *Nature* **2020**, *582*, 55–59. [CrossRef]
22. Dawari, C.K.; Haq, I.; Mönkkönen, K.; Suvanto, M.; Saarinen, J.J. Reduced sliding friction on flat and microstructured metal injection molded (MIM) WC-Co hard metals with MoS_2 composite lubricants. *Tribol. Int.* **2021**, *160*, 107020. [CrossRef]
23. Dawari, C.K.; Mönkkönen, K.; Suvanto, M.; Saarinen, J.J. Solid lubrication on hard metal specimens with micropits under normal and elevated temperatures. *Tribol. Lett.* **2022**, *70*, 30. [CrossRef]
24. Gunell, M.; Haapanen, J.; Brobbey, K.J.; Saarinen, J.J.; Toivakka, M.; Mäkelä, J.M.; Huovinen, P.; Eerola, E. Antimicrobial characterization of silver nanoparticle-coated surfaces by touch test method. *Nanotechnol. Sci. Applic.* **2017**, *10*, 137–145. [CrossRef] [PubMed]
25. Pasquet, J.; Chevalier, Y.; Couval, E.; Bouvier, D.; Noizet, G.; Morlière, C.; Bolzinger, M.-A. Antimicrobial activity of zinc oxide particles on five micro-organisms of the Challenge Tests related to their physicochemical properties. *Int. J. Pharm.* **2014**, *460*, 92–100. [CrossRef] [PubMed]
26. Tayel, A.A.; El-Tras, W.F.; Moussa, S.; El-Baz, A.F.; Mahrous, H.; Salem, M.F.; Brimer, L. Antibacterial action of zinc oxide nanoparticles against foodborne pathogens. *J. Food Saf.* **2011**, *31*, 211–218. [CrossRef]
27. Applerot, G.; Lipovsky, A.; Dror, R.; Perkas, N.; Nitzan, Y.; Lubart, R.; Gedanken, A. Enhanced antibacterial actiwity of nanocrystalline ZnO due to increased ROS-mediated cell injury. *Adv. Funct. Mater.* **2009**, *19*, 842–852. [CrossRef]
28. Yamamoto, O. Influence of particle size on the antibacterial activity of zinc oxide. *Int. J. Inorg. Mater.* **2001**, *3*, 643–646. [CrossRef]